Simulation of Flow over Airfoil

Mangesh Shinde[1], Vishal Shinde[2], Siddhant Shirode[3], Devashish Shriwas[4]

[1-4]Under Graduate Students, Department of Mechanical Engineering, Vishwakarma Institute of Technology, Pune

---***---

Abstract - *The efficiency of an airfoil (NACA 0100-35) is investigated in this report using the finite element analysis process, which uses 2D computational fluid dynamics simulations based on ANSYS to find the lift and drag coefficients under various conditions. The following are the boundary conditions: The airflow velocity is 10m/s, the density is 1kg/m3, the gauge pressure is 0 and the density is 1kg/m3. During the simulation, the Reynolds number is also taken into account. As a consequence, the simulation depicts the airfoil's stalling points and efficiencies at various angles of attack.*

1. Introduction

Given the critical position that aircraft manufacturing has played, the selection of airfoils, which are the section side of airplane wings, should be based on a set of criteria. ANSYS is one of the most commonly used programs in this area, and it is used to obtain accurate results when simulating airfoils. This study aims to look at an airfoil (NACA 0010-35) with various airflow angles using ANSYS and 2D CFD (Computational Fluid Dynamics) simulation. The simulation is necessary to obtain stalling points and efficiencies by determining the values of drag and lift coefficients.

2. Parameters of the Airfoil

2.1 Lift and Drag

Figure 1: Airflow through the airfoil

When an airfoil moves through airflow (as shown in figure 1), an aerodynamic force is produced on it, according to Tom Benson's article[1] (as is showed in figure 2 and figure 3).

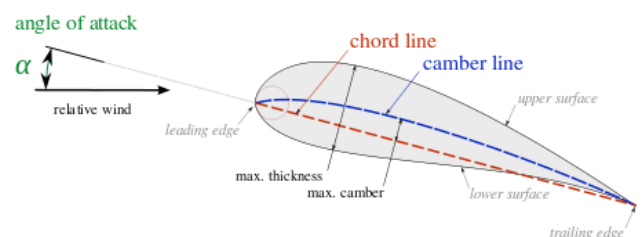The following components make up this aerodynamic force:

$$F = \frac{1}{2} . \rho . C . S . V^2$$

The fluid density is Drag(D) or Lift(L), v is the object's speed relative to the fluid, A is the cross-sectional area, and C_D and C_L are the drag and lift coefficients, respectively.

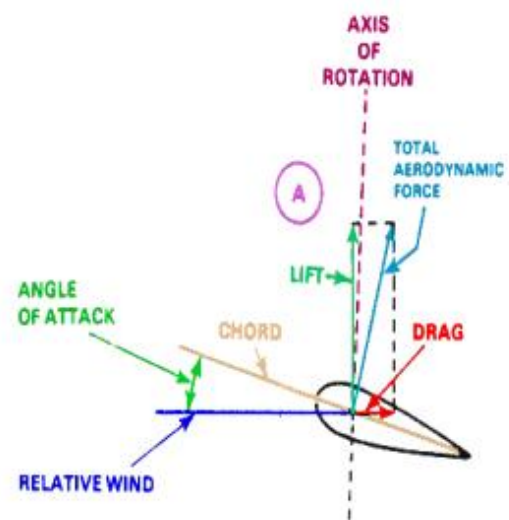**Figure 2: Wing side view (airfoil)**

Figure 3: Lift and Drag forces Vs Angle of Attack

The lift and drag forces on any object are proportionally dependent on the density of the fluid and the relative speed between the object and the fluid, as shown by the equation above.

2.2 Lift and Drag

The equation for the Lift Coefficient, which can be rearranged from the Lift equation, is as follows:

$$C_l = \frac{2L}{\rho v^2 A}$$

Where L is the lift, is the fluid's mass, v is the fluid's velocity, and A is the related surface area [2]. The relevant surface area for the airfoil is a plane shape area [3], which is related to the drag coefficient forms. The lift coefficient is normally calculated experimentally, according to T. Benson [4], but it is a number that can explain all the complex dependencies of form, inclination, and some flow conditions on aircraft lift. This study is based on ANSYS calculations.

Besides, the Drag Coefficient equation can be rearranged as follows from the Drag equation:

$$C_d = \frac{2D}{\rho v^2 A}$$

Where D is the drag force, which is the force factor in the direction of flow velocity, is the fluid's mass density, is the object's speed relative to the fluid and is the reference area.

C_L and C_D could be determined using the ANSYS method in this article.

2.3 Reynolds number

The following equation displays the Reynolds number equation:

$$Re = \frac{\rho v D}{\mu}$$

Where is the airflow density (1kg/m3), v is the airflow velocity (50m/s), D is 1m, and is the air viscosity (1.460e-5).

Patil et al.[5] used CFD analysis to investigate the Lift and Drag forces at different angles of attack for Reynolds numbers ranging from 10,000 to 800,000, and found that the lift and drag forces increased as the Reynolds number increased. Re is 3.42 x 106 in this simulation, as determined by the above equation. As a consequence, the flow is chaotic. Only the relationship between the angle of attack and its consequences is investigated in this case. The angle of attack is the angle formed by the relative wind and the chord, as shown in Figure 3. The angle of attack increases as the leading edge, or front point of the airfoil, rises, which is linked to an increase in lift and drag force [3]. Previous research by Sahin et al. [6] looked into the effect of stalling angle on lift and drag coefficient. Meanwhile, Bhat et al.[7] calculated NACA0012's stalling angle at a specific Reynolds number.

3 Simulation

3.1 Choose an Airfoil

The symmetrical portion of the airfoil NACA 0010-35 was chosen from the UIUC Airfoil Database(n.d.) to simulate (showed in Figure 4).
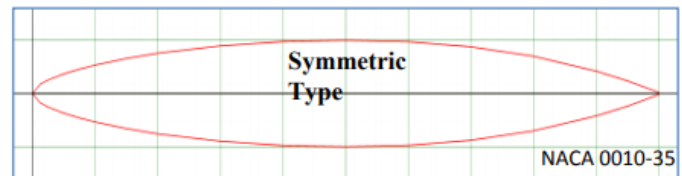

Figure 4: Geometry for NACA 0010-35

Table 1 shows the data that was downloaded from the UIUC Airfoil Database (n.d.) and imported into the ANSYS workbench with Notepad.

Table 1: Data for NACA 0010-35 Airfoil

#Point	X-cord	Y-cord	Z-cord
1	1.00000	0.00100	0.00
2	0.95000	0.01178	0.00
3	0.90000	0.02100	0.00
4	0.80000	0.03500	0.00
5	0.70000	0.04389	0.00
6	0.60000	0.04867	0.00
7	0.50000	0.05000	0.00
8	0.40000	0.04878	0.00
9	0.30000	0.04478	0.00
10	0.20000	0.03789	0.00
11	0.15000	0.03289	0.00
12	0.10000	0.02667	0.00
13	0.07500	0.02289	0.00
14	0.05000	0.01844	0.00
15	0.02500	0.01267	0.00
16	0.01250	0.00878	0.00
17	0.00000	0.00000	0.00
18	0.01250	-0.00878	0.00
19	0.02500	-0.01267	0.00
20	0.05000	-0.01844	0.00
21	0.07500	-0.02289	0.00
22	0.10000	-0.02667	0.00
23	0.15000	-0.03289	0.00
24	0.20000	-0.03789	0.00
25	0.30000	-0.04478	0.00
26	0.40000	-0.04878	0.00
27	0.50000	-0.05000	0.00
28	0.60000	-0.04867	0.00
29	0.70000	-0.04389	0.00
30	0.80000	-0.03500	0.00
31	0.90000	-0.02100	0.00
32	0.95000	-0.01178	0.00
33	1.00000	-0.00100	0.00

3.2 Meshing

The airfoil was sketched in a C-shape domain with a size of 12.5 m for both the semicircle and the rectangle. Figure 5 demonstrates the geometry configuration, with the airfoil in the middle of the figure.
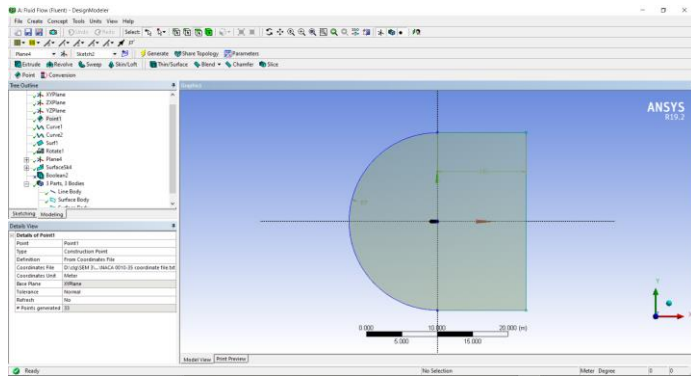

Figure 5: Geometry setup

3.3 Meshing

C-Mesh was added to both airfoils to ensure the model's precision by obtaining a more refined mesh over the trail's edge and the airfoil's surface. The simulation's C-mesh is shown in Figure 6 below:
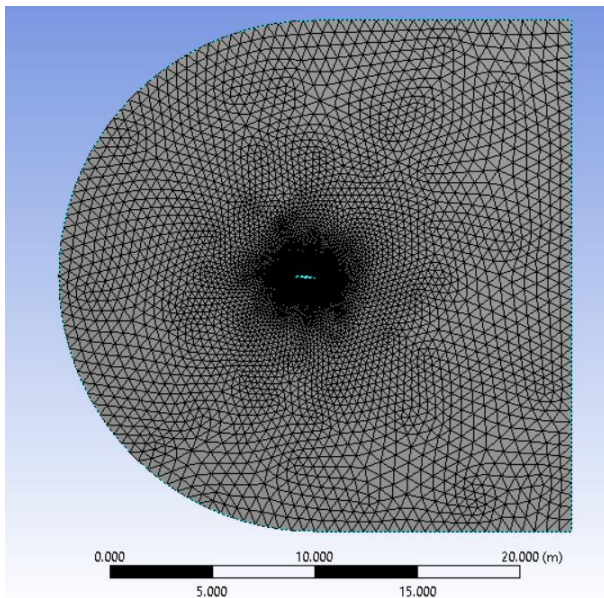

Figure 6: C-mesh

3.4 Set up the test

For the exam, the following settings were used:

Eleni et al. [8] compared various turbulence models, such as Spalart-Allmaras, Realizable k-, and k- shear street transport.

Since it is a simple and popular turbulence model used in industrial applications, the realizable k-ε was chosen.

Fluid air was used as a material in this category.

Boundary conditions zone: Inlet was chosen as the zone condition.

Monitors: The Residual Convergence for the monitors were set to 1e-6.

Second-order upwind was used as the solution process.

Initialization of the solution: The initial values were calculated from the inlet.

Calculation boundary conditions: The following formulas are used to measure the velocity variable in the X and Y directions:

x = [Cos (angle of attack)] * (velocity)

y = [Sin (angle of attack)] * (velocity)

Other options:

- Pressure: 0

- Velocity: 10

- Density: 1

3.5 Run the calculation

Number of Iterations: A total of 1000 iterations were used to ensure that all residuals converged as the angle of attacks increased.

4 Results

More than 30 running tests with various angles of attacks were performed to construct the simulations for the airfoil, as shown in table 4. The lift and drag coefficients, velocity and pressure behaviors against the airfoil, and the effect of airflow over the airfoil will all be shown in the data.

Table 2: Results

Angle of Attack	Inlet Velocity	Drag	Lift	Coefficient of Lift(C_L)	Coefficient of Drag(C_D)	Efficiency (C_L/C_D)
-10	10.0	-48.2165	3.8153	-0.78721	0.07786	-10.11008
-9	10.0	-25.0692	2.2239	-0.40929	0.04538	-9.01831
-8	10.0	-25.2169	2.2068	-0.41170	0.04504	-9.14165
-7	10.0	-23.4177	1.1719	-0.38233	0.02392	-15.98655
-6	10.0	-17.9682	1.1151	-0.29336	0.02276	-12.89117
-5	10.0	-10.1540	0.8789	-0.16578	0.01794	-9.24213
-4	10.0	-1.2204	0.8673	-0.01992	0.01770	-1.12564
-3	10.0	-2.5278	0.7587	-0.04127	0.01548	-2.66544
-2	10.0	7.7662	0.5687	0.12680	0.01161	10.92529
-1	10.0	16.0239	0.4302	0.26161	0.00878	29.79618
0	10.0	11.8693	0.5942	0.19378	0.01213	15.98080
1	10.0	45.1543	0.3145	0.73721	0.00642	114.87415
2	10.0	-12.8597	0.3173	-0.20995	0.00647	-32.42742
3	10.0	-9.7396	0.4537	-0.15901	0.00926	-17.17455
4	10.0	-8.6836	0.3396	-0.14177	0.00693	-20.45408
5	10.0	5.1234	0.8007	0.08365	0.01634	5.11925
6	10.0	10.9244	0.8918	0.17836	0.01820	9.79952
7	10.0	24.2787	1.2402	0.39639	0.02531	15.66115
8	10.0	54.2670	4.2763	0.88599	0.08727	10.15226
9	10.0	75.2381	2.7774	1.22838	0.05668	21.67168
10	10.0	170.9300	16.2488	2.79069	0.33161	8.41564
11	10.0	-28.8089	0.0629	-0.47035	0.00128	-366.34717
12	10.0	38.5732	22.5133	0.62977	0.45946	1.37068
13	10.0	-3.8665	1.4131	-0.06313	0.02884	-2.18895
14	10.0	12.7013	11.0943	0.20737	0.22641	0.91588
15	10.0	28.8381	30.4640	0.47083	0.62171	0.75730
16	10.0	44.4653	14.8096	0.72596	0.30224	2.40197
17	10.0	-14.7504	0.7694	-0.24082	0.01570	-15.33674
18	10.0	-13.1842	1.0354	-0.21525	0.02113	-10.18636
19	10.0	-1.7991	4.0422	-0.02937	0.08249	-0.35606
20	10.0	18.4898	11.1259	0.30187	0.22706	1.32950

4.1 The Airfoil's Maximum Lift Coefficient C_L (Stalling Point)

The angle of attack was increased to achieve the optimal C_L, as seen in the table above (Stalling point). According to the table and figure 7, as the angle of attack increases, the C_L increases as well, until the angle of attack is set to 10, at which point the C_L begins to decrease, and the angle of attack 10 is referred to as the stalling point, where the airfoil's maximum C_L is found.
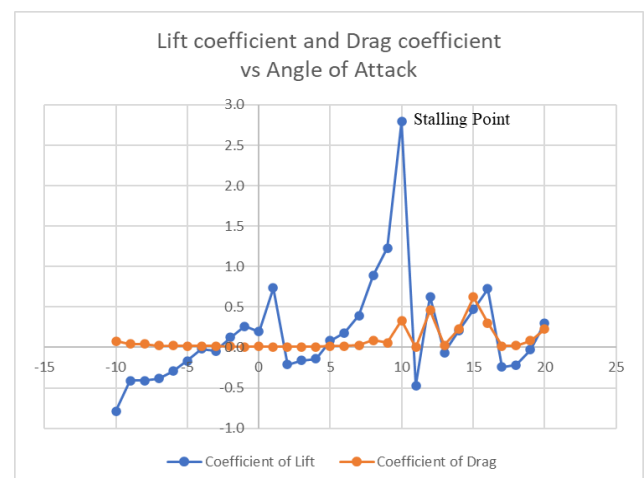

Figure 7: Lift and Drag Coefficients vs Angle of Attacks

4.2 Maximum Efficiency of the Airfoil

Since efficiency is defined as the ratio of C_L to C_D at each angle of attack, it can be seen in figure 8 that the airfoil's maximum efficiency is achieved at an angle of attack (1).
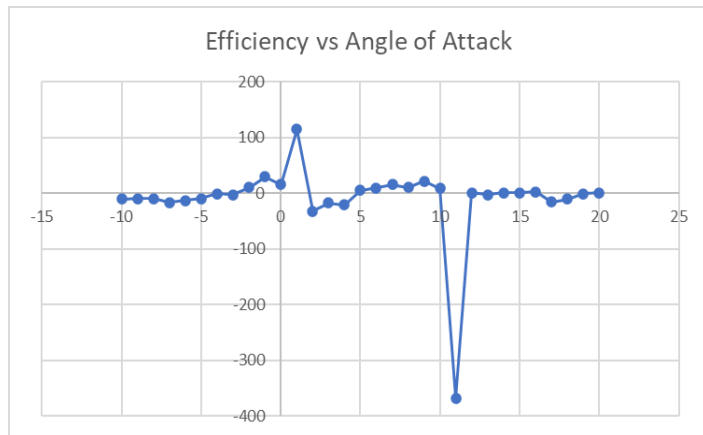

Figure 8: The Efficiency vs Angle of Attack

4.3 Contours of the static pressure of the airfoil

As airfoil1 passes through airflow and the angle of attack increases, the pressure progressively increases and appears on the bottom surface of the airfoil, as shown in the diagrams below (figures 9,10,11,12). According to Bernoulli's theory, the airfoil's upper surface has low pressure while the lower surface has higher pressure, causing the flow to accelerate on the upper surface while decreasing on the lower surface.
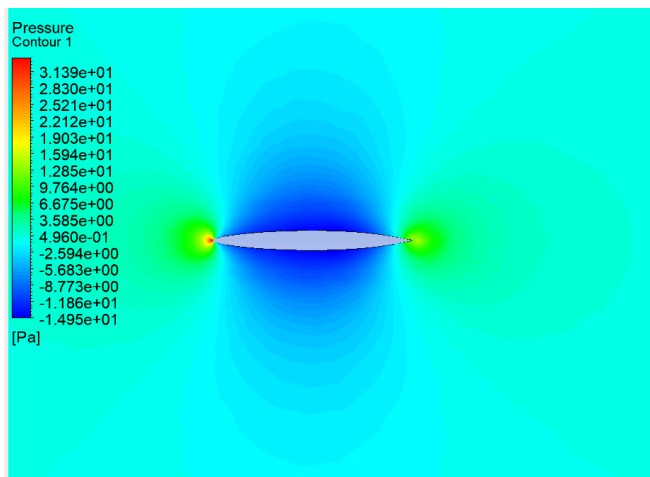
Figure 9: Contours of static pressure (Angle=0)
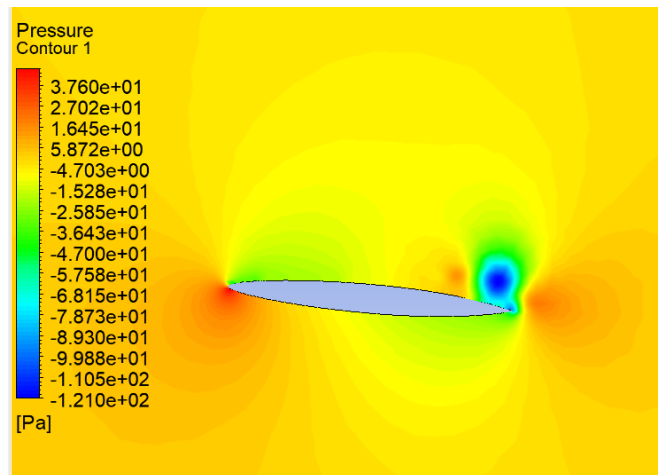
Figure 10: Contours of static pressure (Angle=5)
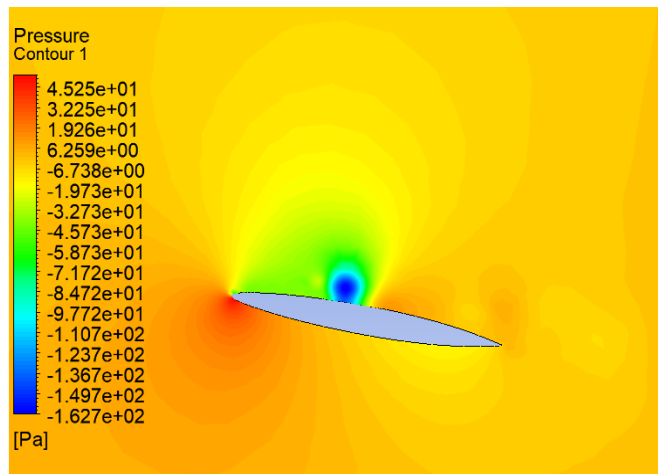
Figure 11: Contours of static pressure (Angle=10)
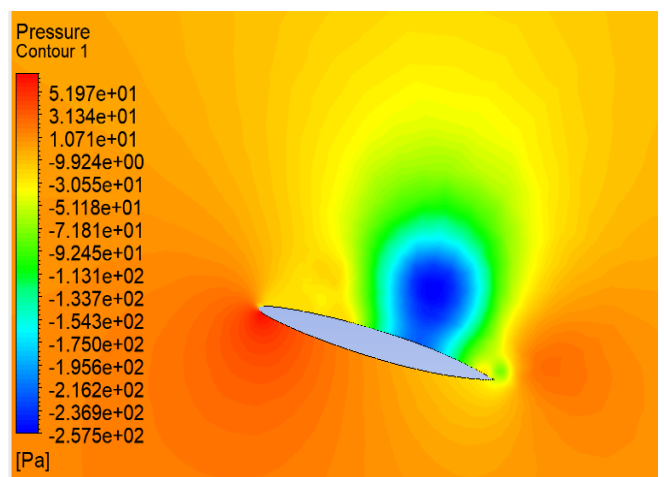
Figure 12: Contours of static pressure (Angle=15)

4.4 Contours of velocity magnitude of the airfoil

When airfoil1 passes through airflow and the angle of attack increases, the velocity progressively increases and appears on the top surface of the airfoil, as shown in the diagrams below (figure 13,14,15,16). As the angle of attack increases after the stalling point, the air separation will also be noticeable.
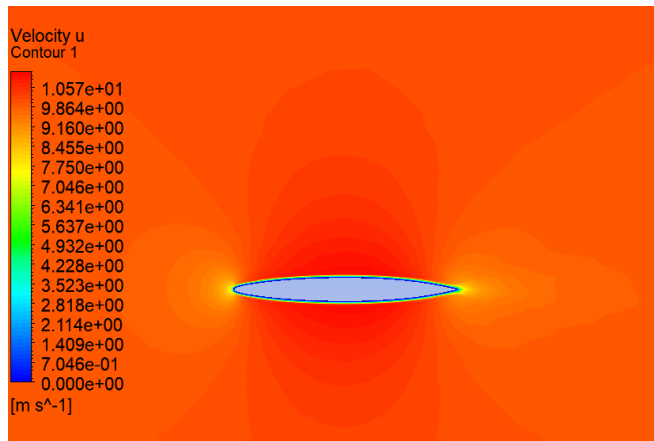

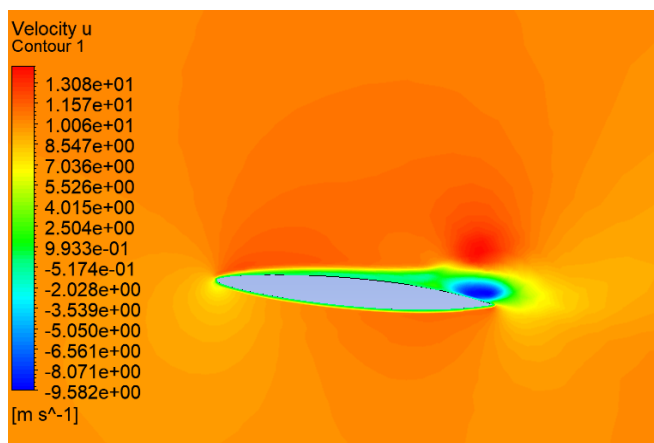**Figure 13: Contours of velocity magnitude (Angle=0)**
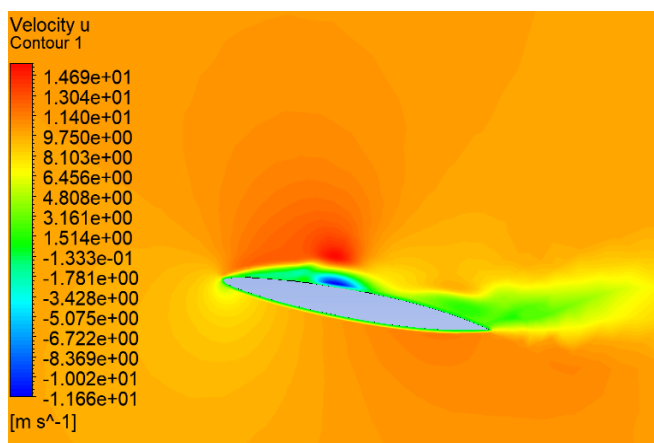

Figure 14: Contours of velocity magnitude (Angle=5)

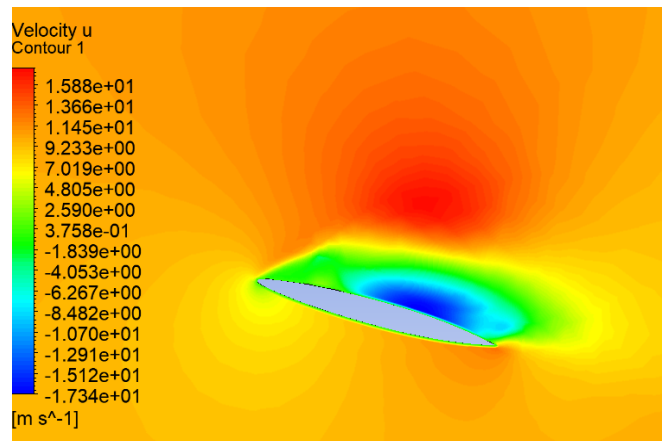**Figure 15: Contours of velocity magnitude (Angle=10)**

Figure 16: Contours of velocity magnitude (Angle=15)

4.5 Velocity Stream Function of the Airfoil

As airfoil1 passes through airflow and exceeds the Full C_L, air separation begins and a vortex forms as the angle of attack increases, as shown in figure 17,18,19,20.
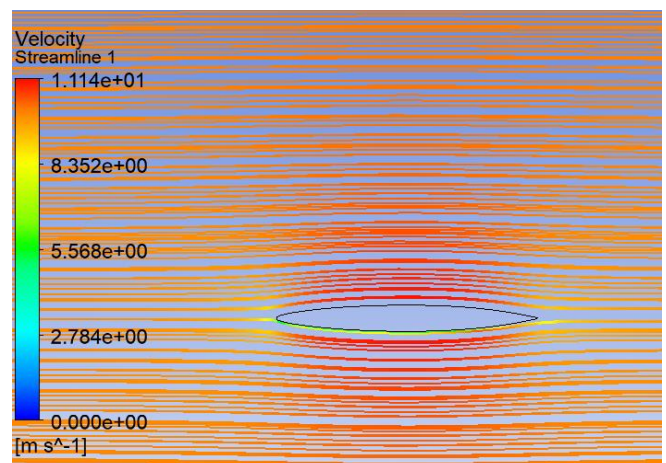

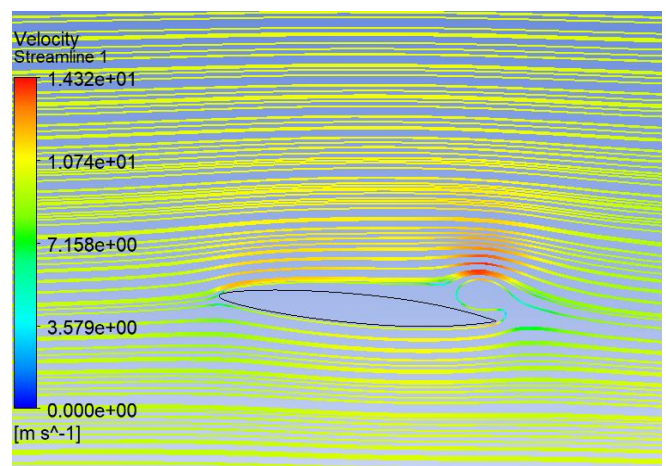**Figure 17: Velocity stream function (Angle=0)**

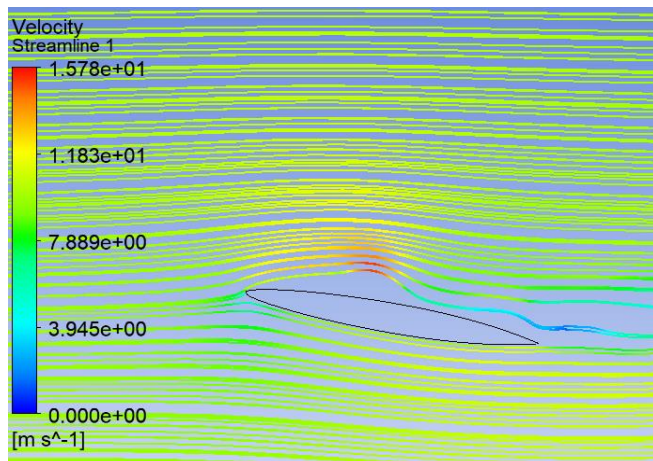**Figure 18: Velocity stream function (Angle=5)**

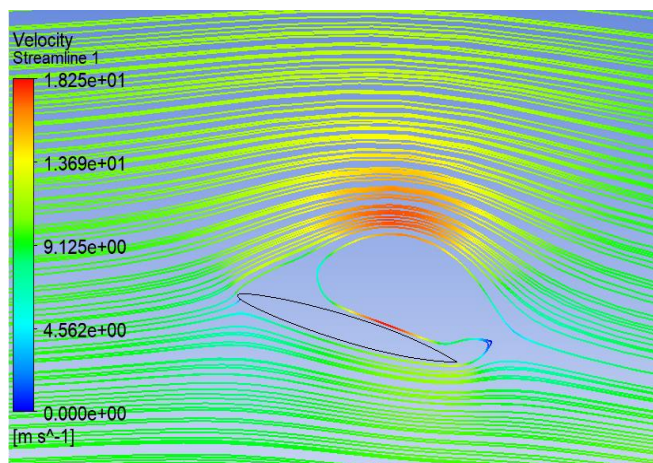**Figure 19: Velocity stream function (Angle=10)**

Figure 20: Velocity stream function (Angle=15)

5 Discussions and Conclusion

ANSYS Workbench fluent software Simulation was used to select and examine this symmetrical airfoil. This study aims to find the airfoil's maximum Lift Coefficient (stalling point) and maximum Efficiency through a series of running calculations at various angles of attack. When all of the results for different angles of attacks are compared, it can be shown that NACA0010- 35 has the stalling point at a 10-degree angle. Since the stalling point is lower, the airfoil will have more time to detach from the air, which will assist in lifting the aircraft. When an airfoil approaches full efficiency with a lower angle of attack, however, it has a higher Maximum Efficiency.

Appendix

The following are the details and geometry for the NACA0010-35 airfoil from the UIUC Airfoil Database: http://m-selig.ae.illinois.edu/ads/coord_database.html#N

REFERENCES

[1] T Benson. National Aeronautics and Space Administration. Aerodynamic Forces, retrieved from http://www.grc.nasa.gov/WWW/k-12/airplane/presar.html (n.d.)

[2] Cited from Wikipedia: http://en.wikipedia.org/wiki/Lift_coefficient

[3] IJER, 3 154-158, K S Patel, S B Patel, U B Patel, et al (2014)

[4] T Benson. National Aeronautics and Space Administration. Aerodynamic Forces, retrieved from http://www.grc.nasa.gov/WWW/k-12/airplane/liftco.html (n.d.)

[5] Procedia Engineering 127 1363–1369, B S Patil, H R Thakare (2015)

[6] International Journal of Materials, Mechanics, and Manufacturing 3 1 (I. Sahin, A. Acir) (2015)

[7] S S Bhat, R N Govardhan. Journal of Fluids and Structures 41 166-174 (2013)

[8] M P Dionissios, D C Eleni, T I Athanasios JMER, vol. 4, no. 3, pp. 100-111 (2012)

[9] Investigation of Flow over the Airfoil, Attack Shiming Xiao, a and Zutai Chen